Inorg. Chem. **2007**, *46*, 3176–3184

Large-Scale, Surfactant-Free, Hydrothermal Synthesis of Lithium Aluminate Nanorods: Optimization of Parameters and Investigation of Growth Mechanism

Upendra A. Joshi and Jae Sung Lee*

Eco-friendly Catalysis and Energy Laboratory (NRL), Pohang University of Science and Technology (POSTECH), San 31 Hyoja-dong, Pohang 790-784, Korea

Received November 22, 2006

Lithium aluminate nanorods were successfully synthesized from Al_2O_3 nanoparticles and lithium hydroxide by a simple, large-scale hydrothermal process without any surfactant or template. The various reaction parameters were optimized to achieve the maximum yield. The as-obtained nanorods had orthorhombic β-lithium aluminate structure with edges in the range of 40–200 nm and lengths of 1–2 μm confirmed by SEM, TEM, XRD, and NMR. Upon calcination at 1273 K for 12 h it transformed to γ-lithium aluminate, yet maintained the initial morphology, demonstrating the thermal stability. The ratio of lithium hydroxide to aluminum oxide showed a significant effect on the morphology as Li/Al = 1 gives "microroses", whereas Li/Al = 3 and Li/Al = 15 gave "microbricks" and "nanorods", respectively. Investigation of the mechanism showed that the nanorods were formed via a "rolling-up" mechanism. As we used all-inorganic raw materials and a simple synthetic procedure under mild conditions, the scale-up of this process for large-scale production should be very easy.

1. Introduction

Lithium aluminate, $LiAlO_2$, is a potential candidate material for the tritium breeder of a fusion reactor[1] or the electrolyte matrix of a molten carbonate fuel cell[2] (MCFC) due to its chemical and thermal stability as well as low radiation damage susceptibility. The capture of a neutron by ^{6}Li is known to occur as follows:

$$^6\mathrm{Li} + {}^1\mathrm{n} \rightarrow {}^4\mathrm{He} + {}^3\mathrm{T}$$

In preparing ceramic materials, it is important to be able to have precise control over the microstructure, since the microstructure is considered to play an important role in controlling tritium release kinetics from the blanket.[3] γ-$LiAlO_2$ doped with Fe emits in the deep-red region rendering it suitable for artificial plant illumination.[4]

Forty years ago, Lehmann and Hesselbarth[5] found that lithium aluminate exists in the two polymorphic forms of α and γ. Lejus and Collongues[6] have determined the crystallographic structure of these phases. The α-form is trigonal with a NaCl-like arrangement elongated along a 3-fold axis, where both cations have octahedral coordination (the coordination number of both cations is 6 with equidistant oxygen neighbors). The structure consists of alternating sheets of LiO_6 and AlO_6 octahedra. The structural group is $R3m$, and the crystallographic density is $d\alpha = 3.401$ g/cm^3. Poeppelmeier et al.[7] have reported the recent values of the lattice parameters of this phase: $a = b = 2.7993$ Å, $c = 14.180$ Å.

The γ-phase is tetragonal with an arrangement similar to that of crystobalite, where all atoms have tetrahedral coordination. Both cations have coordination number 4. The Al atoms are in place of the silicon, and the lithium atoms occupy the tetrahedral holes in the array of the aluminum tetrahedral. The crystallographic parameters of this form are $a = 5.169$ Å and $c = 6.268$ Å, and the crystallographic density is $d\gamma = 2.615$ g/cm^3. These parameters are very

* To whom correspondence should be addressed. E-mail: jlee@postech.ac.kr. Phone: 82-54-279-2266. Fax: 82-54-279-5528.

(1) Loya, A. D.; Carrera, L. M.; Ureña-Núñez, F.; Palacios, O.; Bosch, P. *Appl. Radiat. Isot.* **2003**, *58*, 509.
(2) Terada, S.; Higaki, K.; Nagashim, I.; Ito, Y. *J. Power Sources* **1999**, *83*, 227.
(3) Carrera, L. M.; Jiménez-Becerril, J.; Basurto, R.; Arenas, J.; López, B. E.; Bulbulian, S.; Bosch, P. *J. Nucl. Mater.* **2001**, *299*, 242.
(4) Kutty, T. R. N.; Nayak, M. *Mater. Res. Bull.* **1999**, *34*, 249.
(5) Lehmann, H. A.; Hesselbarth, H. *Z. Anorg. Allg. Chem.* **1961**, *313*, 117.
(6) Lejus, A.-M.; Collongues, R. *C. R. Acad. Sci.* **1962**, *254*, 2005.
(7) Poeppelmeier, K. R.; Chiang, C. K.; Kipp, D. O. *Inorg. Chem.* **1988**, *27*, 4524.

10.1021/ic062227m CCC: $37.00
Published on Web 03/20/2007

similar to those of sodium aluminate γ-$NaAlO_2$. Chang and Margrave[8] have documented the existence of the third allotropic form of $LiAlO_2$, the β phase, where Al shows a mixed, both octahedral (α-phase) and tetrahedral (γ-phase), coordination. The lattice parameters they reported for the monoclinic β-phase with HBO_2 arrangement are $a = 8.147$ Å, $b = 7.941$ Å, $c = 6.303$ Å. Müller et al.[9] studied the ^{27}Al NMR spectra of all three polymorphs of $LiAlO_2$ and confirmed that the β-$LiAlO_2$ had the orthorhombic structure reported by West[10] but not a monoclinic structure. The stability limit of these phases is crucial for fabrication of the MCFC electrolytic matrix or tritium breeding blanket for fusion reactors. The α-form (low-temperature phase) transforms to the γ-form at about 1273 K, while the metastable β-form is assumed to transform to the γ-form at about 1073 K.

The morphology control of ceramic particle is important as it affects the characteristic of the final product. Only a few methods of preparing fibrous lithium aluminate are proposed. A method of filling a micromold fiber with a mixture of lithium and aluminum precursors followed by burning out the micromold was reported.[11] But impurities such as binder and plasticizers were added during mixing of the precursors, and a high temperature was needed for burning the micromold. In the method of drawing fibrous $LiAlO_2$ from a melt, it is difficult to maintain the lithium and aluminum ratio during heating at high temperatures. Needle-shaped β-lithium aluminate was obtained by a solid-state reaction between lithium hydroxide and alumina in alkali hydroxide.[12,13] Li et. al.[14] and Lin et al.[15] produced fine γ-lithium aluminate particles from combustion synthesis in the presence of various fuels. There are a few examples of synthesis of lithium aluminate by the sol−gel process,[16,17] which uses costly metal alkoxide as a precursor. Renoult et al.[18] and Hirano et al.[19] prepared $LiAlO_2$ by hydrolysis of alkoxides of both metals. These routes have potential drawbacks as they use alkoxide precursors, which are costly and very difficult to handle for large-scale synthesis as they hydrolyzed quickly. Jimenez-Becerril et al.[20] and Kinoshita et al.[21] reported the synthesis of lithium aluminate by solid-state reaction using all-inorganic precursors at 973−1073 K. Several attempts have been made to produce rod-shaped particles, but the morphology obtained was in the micrometer scale.[22]

Hydrothermal synthesis has been widely used for the preparation of nanostructured materials and has been shown to be effective in particular for the synthesis of nanowires, nanorods, and nanotubes[23,24] as it has advantages in reducing processing temperature and yielding a nearly site-ordered phase while producing fine crystalline materials. Kwon and Park[25] reported the synthesis of lithium aluminate from the sol−gel process followed by hydrothermal treatment.

Our objective is to develop a simple, large-scale process for the synthesis of lithium aluminate nanorods from all-inorganic precursors without using any organic precursor or surfactant, to make the synthesis process more economic. Recently, we reported the surfactant-free hydrothermal synthesis of lithium aluminate microbricks and nanorods as a preliminary communication.[26] In continuation of the work, we describe in this paper the effect of various synthesis parameters such as lithium precursor, hydrothermal temperature, time, and calcination temperature on morphology. Furthermore, we investigated the mechanism for the formation of nanorods.

2. Experimental Section

2.1. Synthesis of Materials. All chemicals were obtained from Aldrich and used as is without further purification. In the typical synthesis of lithium aluminate nanorods, 0.15 mol (3.59 g) of LiOH and 0.0098 mol (1 g) of Al_2O_3 nanopowder were stirred together with 36 mL of distilled water for 1 h. Then the mixture was transferred to a Teflon-lined reactor (100 mL) and was put into hydrothermal reaction at a constant temperature (423 K) without disturbing it for 3 days. The as-obtained white product was separated by centrifugation, washed with distilled water to remove excess of LiOH, and then dried in an oven at 373 K for 12 h. A similar procedure was employed to investigate the effect on morphology of various lithium precursors such as lithium acetate, lithium nitrate, lithium carbonate, and lithium chloride. To investigate the effect of Li/Al molar ratio and hydrothermal temperature, we varied the concentration (Li/Al = 3, 5, 12, and 15) and temperature (353, 373, 393, 423, and 453 K). The calcination of as-obtained product was carried out in a quartz reactor under an air flow of 136 μmol/s at various temperatures of 773, 973, 1073, 1173, and 1273 K.

2.2. Characterization of Materials. X-ray diffraction (XRD) patterns were obtained on a MAC-Science M18XHF diffractometer with Cu Kα radiation (40 kV, 200 mA). The scanning electron microscopy (SEM) analyses were carried out to see the overall morphology of the samples on FE-SEM, FEI XL30S with an accelerating voltage of 3 kV. The transmission electron microscope (TEM) samples were prepared by dispersing the material in ethanol using ultrasonication and dropping it onto a holey carbon film supported on a copper grid and drying in an oven at 353 K. The low-magnification TEM images were taken on a Philips CM-30

(8) Chang, C. H.; Margrave, J. L. *J. Am. Chem. Soc.* **1968**, *90*, 2020.
(9) Müller, D.; Gessner, W.; Scheler, G. *Polyhedron* **1983**, *2*, 1195.
(10) West, A. R. *Z. Kristallogr.* **1975**, *141*, 422.
(11) Fain, C. C.; Lowe, G. M.; Frianeza-kullberg, T. N.; McDonald, D. P. Patent WO 94/03409, February 17, 1994.
(12) Watnabe, A.; Takeuchi, Y.; Saeki, G. *J. Am. Ceram. Soc.* **1987**, *70*, C268.
(13) Saeki, G.; Watanabe, A. *J. Ceram. Soc. Jpn.* **1992**, *100*, 1421.
(14) Li, F.; Hu, K.; Li, J.; Zhang, D.; Chen, G. *J. Nucl. Mater.* **2002**, *300*, 82.
(15) Lin, W.; Bai, X.; Ling, Y.; Yang, J.; Ma, W. *J. Mater. Sci.* **2003**, *38*, 3883.
(16) Oksuzomer, F.; Koc, S. N.; Boz, I.; Gurkaynak, M. A. *Mater. Res. Bull.* **2004**, *39*, 715.
(17) Valenzuela, M. A.; Téllez, L.; Bosch, P.; Balmori, H. *Mater. Lett.* **2001**, *47*, 252.
(18) Renoult, O.; Boilot, J.-P.; Boncoeur, M. *J. Am. Ceram. Soc.* **1994**, *77*, 249.
(19) Hirano, S.-I.; Hayashi, T.; Kageyama, T. *J. Am. Ceram. Soc.* **1987**, *70*, 171.
(20) Jimenez-Becerril, J.; Bosch, P.; Bulbulian, S. *J. Nucl. Mater.* **1991**, *185*, 304.
(21) Kinoshita, K.; Sim, J. W.; Ackerman, J. P. *Mater. Res. Bull.* **1978**, *13*, 445.
(22) Kim, S.-D.; Hyun, S.-H.; Lim, T. H.; Hong, S. A. *J. Power Sources* **2004**, *137*, 24.
(23) Xia, Y.; Yang, P.; Sun, Y.; Wu, Y.; Mayers, B.; Gates, B.; Yin, Y.; Kim, F.; Yan, H. *Adv. Mater.* **2003**, *15*, 353.
(24) Joshi, U. A.; Lee, J. S. *Small* **2005**, *1*, 1172.
(25) Kwon, S. W.; Park, S. B. *J. Mater. Sci.* **2000**, *35*, 1973.
(26) Joshi, U. A.; Chung, S. H.; Lee, J. S. *Chem. Commun.* **2005**, *35*, 4471.

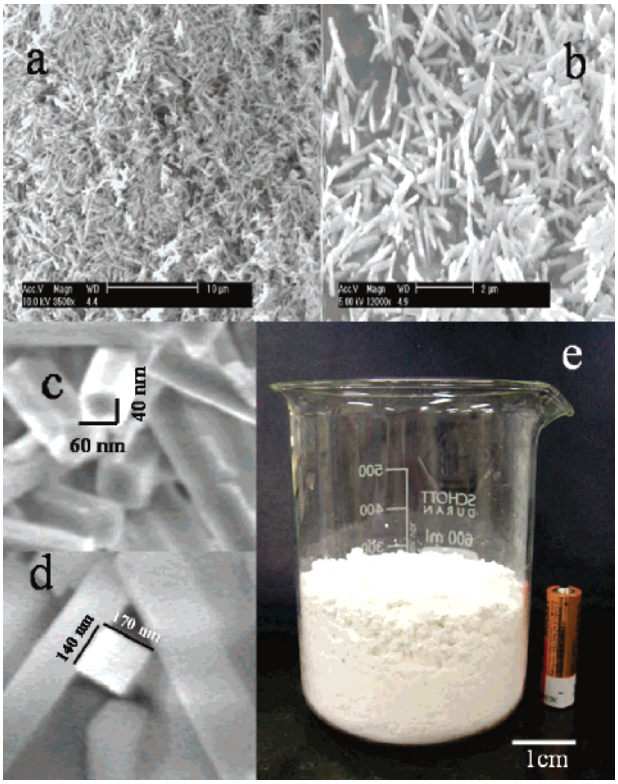

Figure 1. (a) Low-magnification SEM image of as-obtained nanorods (bar scale 10 μm). (b) A high-magnification SEM image further confirms that nanorods have edges in the range of 40−200 nm and lengths of 1−2 μm (bar scale 2 μm). (c and d) Typical cross sections of nanorods showing a rectangular shape. (e) $LiAlO_2$ nanorods produced in a large scale. A typical batch size is 100 g. The AA battery cell is shown for comparison of dimension.

instrument operated at 200 kV. Similarly, the field emission, high-resolution electron microscope (FE-HREM) images and corresponding selected area electron diffraction (SAED) patterns were obtained on a JEOL JEM 2010F instrument equipped with a Gatan imaging filter (GIF) system operated at 200 kV. The ^{27}Al solid-state NMR measurements were performed on a Varian Unity Inova 300 MHz spectrometer (7.4 T) equipped with a 7 mm Chemagnetics MAS probe head using a sample rotation rate of 5.5 kHz. The ^{27}Al MAS NMR spectra were obtained at a frequency of 78.156 MHz. The chemical shifts for ^{27}Al were referred to the position of $Al(H_2O)_6^{3+}$ from an $AlCl_3$ aqueous solution.

3. Results and Discussion

3.1. Surfactant-Free Hydrothermal Synthesis of $LiAlO_2$ Nanorods. Hydrothermal treatment (at 423 K for 3 days) of aluminum oxide nanoparticles with lithium hydroxide in the absence of any surfactant produces uniform rod-shaped morphology as shown in Figure 1a. Further confirmation of the uniformity in morphology and size can be found in a high-magnification SEM image presented in Figure 1b. Figure 1c shows the cross section of the as-obtained nanorods, which clearly shows that the nanorods do not have a circular cross section but a rectangular one. More evidence of the rectangular cross section can be found in Figure 1d. These nanorods are typically 1−2 μm in length, and the edges are in the range of 40−200 nm. According to definition, nanorods are structures with a width of 1−100 nm and an aspect ratio (major axis/minor axis) less than 20,

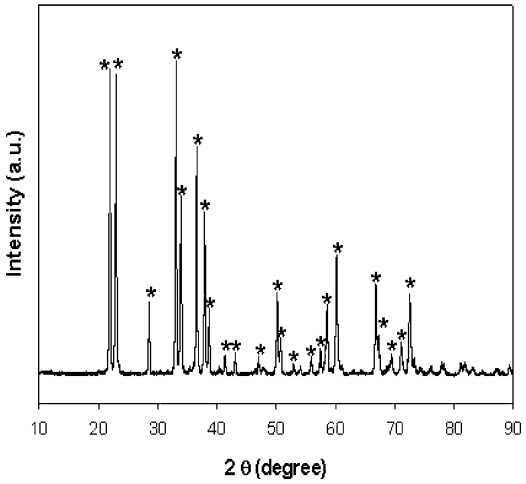

Figure 2. XRD pattern of as-obtained nanorods. The highly crystalline peaks of orthorhombic β-lithium aluminate are shown by an ∗.

while nanowires are analogous structures with an aspect ratio greater than 20.[27] As the product obtained here has an aspect ratio of ∼10 and cross sections of these nanorods are rectangular, we could call them "rectangular nanorods". Typically by this process we can produce 100 g of nanorods as shown in Figure 1e. Hence, this proves that our process is easy to scale-up for large-scale production.

An X-ray diffraction study was carried out to find out the structure of the as-obtained lithium aluminate nanorods. Figure 2 shows the typical X-ray diffraction pattern of the lithium aluminate nanorods, which confirms that the as-obtained nanorods are crystalline, phase pure, and have the orthorhombic β-polymorph. The unit cell parameters for these orthorhombic β-lithium aluminate nanorods were determined to be $a = 5.3$ Å, $b = 6.3$ Å, and $c = 4.9$ Å, which are in agreement with the corresponding bulk materials (space group symmetry $Pna2_1$ (33), JCPDS 33-0785).

In order to investigate the structural environment of Al atom in our nanorods, we carried out ^{27}Al MAS NMR. Figure SI-1 in the Supporting Information presents the NMR spectrum of the lithium aluminate nanorods. The sharp peak at 79.28 gives clear evidence of the tetrahedral coordination of the Al in $LiAlO_2$. As we do not observe any chemical shift due to octahedrally coordinated Al nuclei it is confirmed that our lithium aluminate nanorods are not in the monoclinic structure but instead have the orthorhombic structure reported by Müller et al.[9] and West.[10]

Representative TEM images are shown in Figure 3. From Figure 3a, it is evident that the nanorods have fairly uniform lengths of 1−2 μm and diameters of 40−200 nm. In particular, no irregular branching or bending is observed, which implies that the $LiAlO_2$ nanorods grow in 1D with high crystal perfection. It is important to note that we obtained nanorods without using any surfactant or template. The inset of Figure 3a shows a side view of the tip of a nanorod. These results are consistent with those of SEM. In order to study the lattice structure and to judge the growth direction of β-$LiAlO_2$ rectangular nanorods, an HRTEM

(27) Murphy, C. J.; Jana, N. R. *Adv. Mater.* **2002**, *14*, 80.

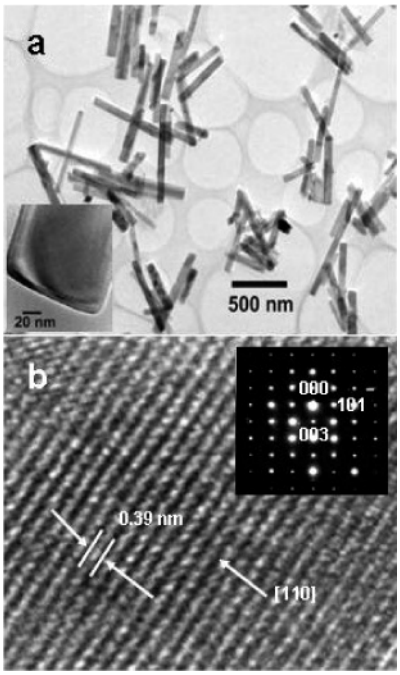

Figure 3. (a) Typical TEM image shows that the lengths of nanorods are in the range of 1−2 μm, whereas the widths are 40−200 nm. The inset shows the side view of a nanorod. (b) HR-TEM image clearly shows the lattice fringes of the (110) plane. The inset shows a selected area electron diffraction pattern.

experiment was carried out. On the basis of the calculation of the lattice spacing and an analysis of its orientation, it was found that the nanorods grew perpendicular to [110]. The inset of Figure 3b shows the corresponding selected area electron diffraction (SAED) pattern.

To investigate the influence of various parameters such as lithium precursors, hydrothermal temperature, and calcination temperature on the morphology, we carried out the same hydrothermal reaction under different conditions.

3.2. Effect of the Lithium Precursor on the Morphology. Hydrothermal treatments (at 423 K for 3 days) of aluminum oxide nanoparticles with various lithium precursors were carried out to find out their effect on the morphology of the lithium aluminate. Figure 4 presents the SEM images of the as-obtained product of the hydrothermal reaction. Figure 4a shows the lump-type morphology obtained by the hydrothermal reaction of lithium acetate and aluminum oxide nanoparticles. It should be note that there is no particular morphology observed in this sample. Figure 4b shows the product obtained by the hydrothermal reaction of lithium chloride and aluminum oxide nanoparticles. In this case, we could not find any particular morphology either. Further hydrothermal treatment of lithium carbonate and aluminum oxide nanoparticles gives the platelike morphology as shown in Figure 4c. The same reaction with the lithium nitrate and aluminum oxide gives very fine particles. It is observed from Figure 4d, that the particles do not have uniform morphology. Finally, hydrothermal reaction of lithium hydroxide and aluminum oxide nanoparticles gives the rod-shaped morphology as shown in Figure 4, parts e and f.

It is important to note that only lithium hydroxide gives the uniform rod-shaped morphology as shown in Figure 4,

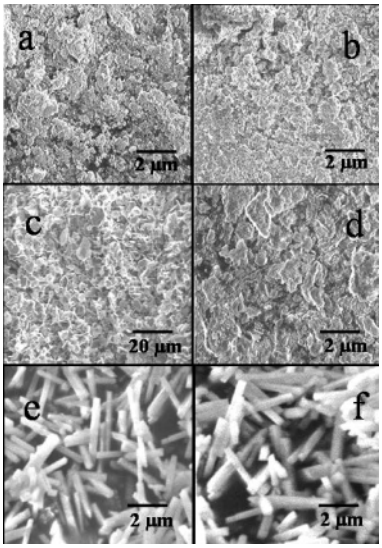

Figure 4. SEM images of the products obtained by the hydrothermal reaction of aluminum oxide with (a) lithium acetate, (b) lithium chloride, (c) lithium carbonate, (d) lithium nitrate, (e and f) lithium hydroxide from a different area of the same sample.

parts e and f, in spite of exactly the same hydrothermal conditions. This clearly shows that there must be a vital role of the anion in the growth of the nanorods. In the literature, Filankembo et al.[28] studied the effect of various salts on the morphology and growth of the copper nanocrystals. They reported that, even through they used a template for the control of the morphology, addition of the chloride ion remarkably change the morphology of the product. In another report, Kwon and Park[25] did a similar study to find out the effect of the precursor on the morphology of lithium aluminate.

They carried out the sol−gel reaction followed by the hydrothermal process of various lithium and aluminum precursors and found that the lithium nitrate precursor gave the platelike morphology, whereas in our study we obtained the similar morphology with the lithium carbonate precursor. Hence, it is clear that anions also have an important role in the crystal growth and morphology. To identify the crystal phase of all the hydrothermal products, we carried out X-ray diffraction analysis. Figure 5 shows the typical X-ray diffraction patterns of the hydrothermal reaction products with the various lithium precursors. XRD pattern a in Figure 5 shows the β-$LiAlO_2$ phase obtained by the reaction of lithium hydroxide and aluminum oxide. Hydrothermal reaction of lithium acetate and aluminum oxide gives the mixture of Al_2O_3 and lithium acetate (indicated by "o"). It should be noted that the peak intensity is very low showing that the phase is not crystalline. Further hydrothermal reaction of lithium chloride and aluminum oxide forms the $LiAl_2(OH)_7{\cdot}2H_2O$ (JCPDS 40-0710) phase as indicated by pattern c in Figure 5. A mixture of lithium carbonate (indicated by an $*$ in Figure 5d) and lithium aluminum oxide carbonate hydrate (JCPDS 37-0625) is obtained by the hydrothermal reaction of lithium carbonate and aluminum oxide. Finally,

(28) Filankembo, A.; Giorgio, S.; Lisiecki, I.; Pileni, M. P. *J. Phys. Chem. B* **2003**, *107*, 7492.

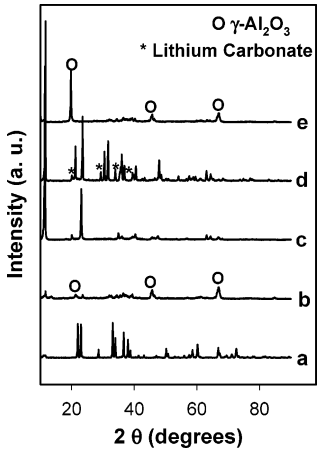

Figure 5. XRD pattern of the products obtained by hydrothermal reaction of aluminum oxide nanoparticles with various lithium precursors: (a) lithium hydroxide, (b) lithium acetate, (c) lithium chloride, (d) lithium carbonate, and (e) lithium nitrate.

reaction between lithium nitrate and aluminum oxide also gives a mixture of aluminum oxide and lithium nitrate. Thus, only lithium hydroxide yields lithium aluminate of high phase purity.

Poeppelmeier and Hwu[29] prepared a precursor via salt imbibition of lithium dialuminate $[LiAl_2(OH)_6]^+(OH)^-\cdot 2H_2O$ and $LiOH\cdot H_2O$ to give Li/Al = 1:1. After calcination of this precursor at 400 °C for 100 h they obtained α-$LiAlO_2$.[7] The main disadvantage of this route is that it required a very long time. The product obtained in our procedure is β-$LiAlO_2$ nanorods, without any surfactant or high-temperature calcination.

3.3. Effect of Lithium Hydroxide to Aluminum Oxide Molar Ratio on the Morphology. As we explained in the section 3.2, only lithium hydroxide gives the rod-shaped morphology. To study the effect of lithium to aluminum oxide molar ratio on the morphology, we carried out the hydrothermal reaction of various amounts of lithium hydroxide with aluminum oxide. The results are shown in the form of SEM images in Figure 6. A Li/Al ratio of 1 gives the flower-type morphology as shown in Figure 6a. These flowers are typically 20 μm in size and look like roses; hence, we call them "microroses". Further evidence of this type of morphology can be observed in Figure 6b, where a number of microroses are aligned on one another like a bouquet. We believe that these roses are formed due to spiral crystal growth controlled by screw dislocations, which is a typical text book example.[30] Figure 6, parts c and d, shows SEM images of the products from synthesis with Li/Al = 3. From the SEM it is clear that the morphology of the as-obtained product looks like bricks. As the typical length is 25−27 μm and the edges are 8−9 μm, we called them "microbricks". The uniformity of the microbricks is impressive over a wide area as shown in the Supporting Information (Figure SI-2). Further synthesis with Li/Al = 7 and Li/Al = 10 gives a mixture of nanorods and particles as shown in Figure 6, parts e and f. When we change the Li/Al ratio to 15 we obtained uniform nanorods, as presented in Figure 6, parts g and h.

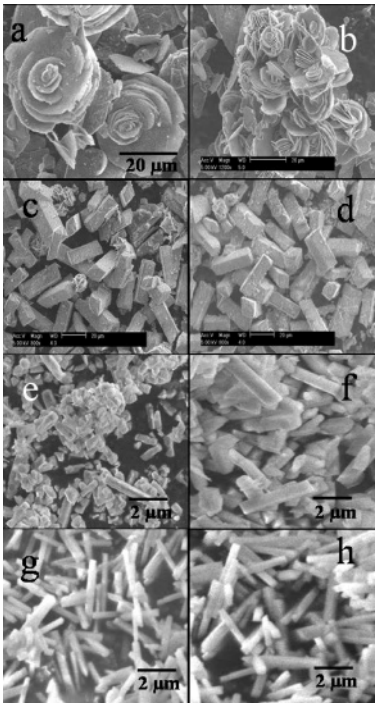

Figure 6. SEM images of products obtained from the hydrothermal reaction of aluminum oxide nanoparticles with various mole ratios of lithium hydroxide: (a and b) Li/Al = 1, (c and d) Li/Al = 3, (e) Li/Al = 7, (f) Li/Al = 10, (g and h) Li/Al = 15.

It is interesting to note that only Li/Al = 15 gives the nanorods and ratios of 2 and 3 give the microroses and microbricks, respectively. Wang and Li[31] reported the synthesis of lanthanide hydroxide single-crystal nanowires from lanthanide oxide dissolved in concentrated nitric acid and reprecipitated by KOH. They observed a significant pH effect, as pH = 6−7 gave sheets, pH = 9 gave nanowires, and pH = 14 also gave nanowires, but in decreased aspect ratio. A higher pH value implies a higher OH^- ion concentration and a higher chemical potential in solution. A higher chemical potential is preferable for the growth of nanowires or nanorods. Thus, when we use excess LiOH which produces higher OH^- ion concentrations and hence higher chemical potential reset, the nanorod morphology is obtained. But in the absence of this excess OH^- ion, further crystal growth yields microbricks. Further decrease in OH^- concentration gives a curved sheetlike morphology, which happens to look like roses. This shows that the lithium hydroxide concentration can have a critical effect on the morphology of the product. X-ray analyses of all the products were carried out to find out the phases. It is seen from Figure 7 that the product obtained from the hydrothermal reaction with Li/Al =1 is lithium aluminate hydrate ($Li_2Al_2O_4$, JCPDS 01-1306, pattern a). Although the peak intensity is different from the reference, all the peak positions match well with that of $Li_2Al_2O_4$, whereas microbricks and nanorods are β-$LiAlO_2$ (pattern b and e). X-ray diffraction patterns c and

(29) Poeppelmeier, K. R.; Hwu, S.-J. *Inorg. Chem.* **1987**, *26*, 3297.
(30) Mullin, J. W. *Crystallization*, 3rd ed.; Butterworth-Heinemann: Oxford, 1997.
(31) Wang, X.; Li, Y. *Angew. Chem., Int. Ed.* **2002**, *41*, 4790.

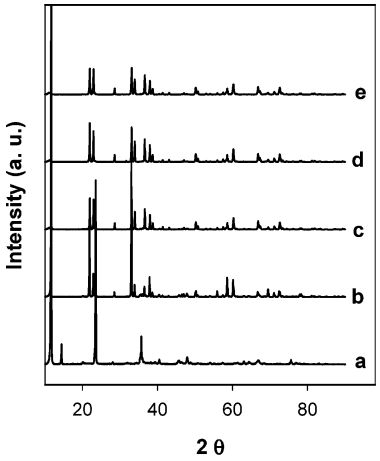

Figure 7. XRD pattern of the products obtained from the hydrothermal reaction of aluminum oxide nanoparticles with lithium hydroxide at different Li/Al mole ratios: (a) Li/Al = 1, (b) Li/Al = 3, (c) Li/Al = 7, (d) Li/Al = 10, and (e) Li/Al = 15.

Table 1. Effects of the Li/Al Ratio on Structure and Morphology

lithium hydroxide to aluminum oxide molar ratio (Li/Al)	XRD phase	morphology
1	lithium aluminate hydrate ($Li_2Al_2O_4 \cdot xH_2O$)	microroses
3	β-$LiAlO_2$	microbricks
7	β-$LiAlO_2$	particles + nanorod
10	β-$LiAlO_2$	particles + nanorod
15	β-$LiAlO_2$	nanorods

d shows that products obtained by the Li/Al molar ratios of 7 and 10 also represent the β-$LiAlO_2$ phase. Table 1 summarizes the morphology and crystal phases observed for various Li/Al ratios. Thus, we can tailor the morphology from microbricks to nanorods just by changing the Li/Al ratio and still maintain the same phase, β-$LiAlO_2$. The morphology control could be very important for the various applications. Furthermore, as we do not use any surfactant or template, scale-up of this process for large-scale production should be very easy.

3.4. Effect of Hydrothermal Temperature on the Morphology. The SEM images in Figure 8 show the effect of hydrothermal temperature on morphology of the product obtained. Figure 8a shows a mixed morphology of plates and big particles obtained by hydrothermal reaction at 353 K. Figure 8b shows the platelike morphology obtained by the same reaction at 373 K. It should be noted that the sample is made of thin hexagonal plates with a typical size of 20 μm. Further SEM images showing the uniformity in the sample are represented in the Supporting Information (Figure SI-3). Figure 8c shows a mixture of nanorods and particles obtained by the hydrothermal reaction at 393 K. The similar reaction at 423 K gives very uniform nanorods as shown in Figure 8, parts d and e. Further increase in hydrothermal temperature to 453 K forms an agglomeration of nanorods as shown in Figure 8f. It seems that this agglomeration occurs to achieve the structural stability. Table 2 summarizes the information about the morphology obtained at various hydrothermal temperatures. From these results we can conclude that the optimum temperature for the hydrothermal

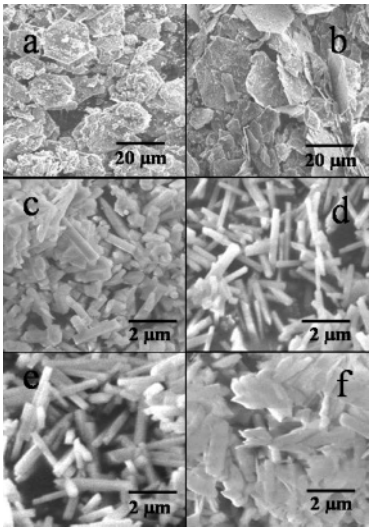

Figure 8. SEM images showing the effect of hydrothermal temperature on the morphology: (a) 353, (b) 373, (c) 393, (d and e) 423, and (f) 453 K.

Table 2. Effects of Hydrothermal Temperature on the Structure and Morphology

hydrothermal temp (K)	XRD phase	morphology
353	$LiOH + LiAl_2(OH)_7 \cdot 2H_2O$	hexagonal plates + particles
373	$LiAl_2(OH)_7 \cdot 2H_2O$	plate-type
393	β-$LiAlO_2$	particles + nanorod
423	β-$LiAlO_2$	nanorod
453	β-$LiAlO_2$	agglomerated nanorods

reaction should be 423 K, as this temperature gives only uniform nanorods.

X-ray analysis results are shown in Figure 9. From the XRD patterns of Figure 9, parts a and b, it can be concluded that the phases formed at the hydrothermal temperature 353 and 373 K are a mixture of LiOH and $LiAl_2(OH)_7 \cdot 2H_2O$ and pure $LiAl_2(OH)_7 \cdot 2H_2O$, respectively. It seems that LiOH reacts with Al_2O_3 to form $LiAl_2(OH)_7 \cdot 2H_2O$ at 353 K, and as the reaction temperature increases to 393−423 K, it is converted to the β-$LiAlO_2$ phase as shown in Figure 9, parts c and d. By further increase in the hydrothermal temperature from 423 to 453 K we obtained β-$LiAlO_2$ as the major phase and $Li_2Al_2O_4$ as the minor phase as shown in Figure 9e.

3.5. Effect of Calcination Temperature on the Morphology and Thermal Stability. As-obtained lithium aluminate nanorods are calcined at various temperatures (773, 973, 1073, 1173, and 1273 K) under air flow. The effect of calcination on the morphology of the nanorods can be clearly observed in the SEM images in Figure 10. Figure 10a shows the morphology of the sample calcined at 773 K, which indicates that there is not much change in the morphology. The XRD pattern (Figure 11 a) shows the β-phase for this sample. The intensity of the peak slightly increased as compared with that of the as-obtained sample. The calcination at 973 K also shows similar results as represented by SEM images in Figure 10b and Figure 11b. Figure 10c shows the SEM images of the sample calcined at 1073 K. The XRD pattern in Figure 11c for this sample shows a mixture of β- and γ-phases. However, the peak intensity of the γ-phase is very small compared to that of the β-phase. It seems that

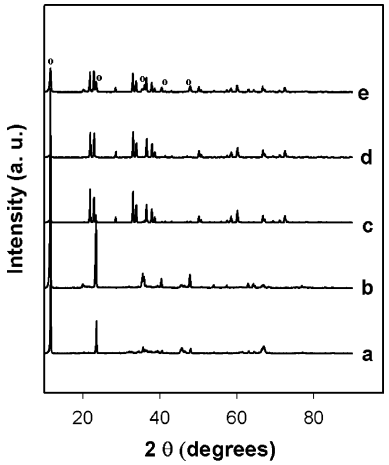

Figure 9. XRD pattern of the products obtained from hydrothermal reaction of lithium hydroxide and aluminum oxide nanoparticles at various hydrothermal temperatures: (a) 353, (b) 373, (c) 393, (d) 423, and (e) 453 K. The "o" in pattern e shows the minor $Li_2Al_2O_4$ phase.

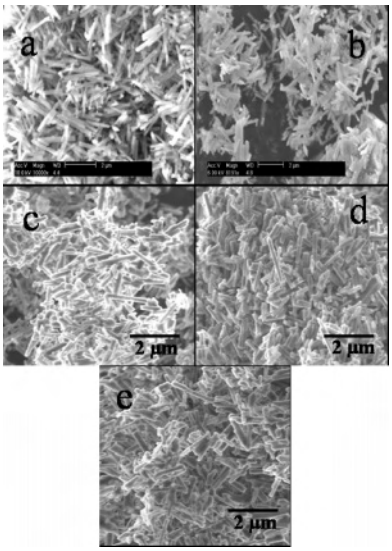

Figure 10. SEM images of the nanorods calcined at various temperatures for 12 h: (a) 773, (b) 973, (c) 1073, (d) 1173, and (e) 1273 K.

the β-phase transforms slowly to the γ-phase. Further calcination at 1173 K (Figure 11d) shows the majority of γ-phase peaks, and the β-phase totally vanishes (also Supporting Information Figure SI-4 clearly shows this difference). It is important to note that the morphology of the nanorods is still maintained as shown in Figure 10d although a few nanorods (<10%) are broken to small particles. Calcination at 1273 K for 12 h gives the phase-pure γ-lithium aluminate as shown in the XRD pattern of Figure 11e. The morphology change in this sample is not much; most of the nanorods (>90%) still maintain their morphology. Interestingly, when we calcined our microroses sample ($Li_2Al_2O_4$) at 500 °C for 10 h we obtained α-$LiAlO_2$. In the literature many reports showed the synthesis of α-$LiAlO_2$ via equimolar mixture of lithium and aluminum precursor. For example Poeppelmeier et al.[7] also reported the synthesis of high surface area α-$LiAlO_2$ by calcination of a lithium dialuminate and lithium hydroxide mixture. Here we obtained the same α-$LiAlO_2$ phase after calcination of a $Li_2Al_2O_4$ precursor.

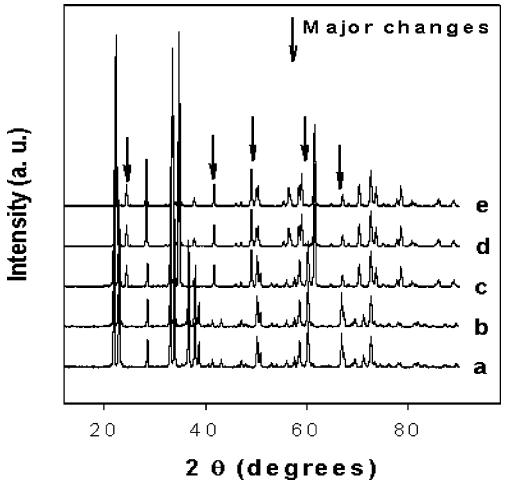

Figure 11. XRD pattern of samples calcined at different temperatures: (a) 773, (b) 973, (c) 1073, (d) 1173, and (e) 1273 K. It should be noted that pattern c shows the peaks for the β-phase as well as the γ-phase. These changes are denoted by arrows.

Ribeiro et al.[32] studied the influence of heat treatment on the structural properties of lithium aluminate. They prepared the γ-lithium aluminate at 1023 K by the sol−gel process. A mixture of γ-lithium aluminate and $LiAl_5O_8$ transformed to γ-$LiAlO_2$ at 1073 K. Similarly, Hirano et al.[19] reported the transformation of β-$LiAlO_2$ to γ-$LiAlO_2$ at 1023 K. They observed that the transformation of β-$LiAlO_2$ to γ-$LiAlO_2$ took place at a lower temperature by 473 K than that of α-$LiAlO_2$ to γ-$LiAlO_2$. The β-to-γ transformation as previously studied by West[9] may takes place by a simple topotactic mechanism. The reason we did not observe any morphology change in the thermally treated nanorods may be the smooth transformation from β-phase to γ-phase (topotactic) with minimal atomic rearrangement, which would not disrupt the initial morphology.[33] In contrast, α-phase to γ-phase transformation requires important structural modifications which may cause instability in the structure and morphology. Thus, the thermal stability of $LiAlO_2$ depends on its phase.

3.6. Investigation of the Formation Mechanism of Lithium Aluminate Nanorods. To investigate the formation mechanism of nanorods, a hydrothermal experiment was carried out while aliquots of reaction mixture were taken at a regular time intervals of 12 h. The SEM images obtained by these experiments are shown in Figure 12. As shown in Figure 12a the agglomeration of particles with fibrous morphology was observed after the reaction time of 12 h. After 24 h the fibers grew to form dendrite nanostructures. It is interesting to note that these dendrites are made up of hexagonal sheets as shown in Figure 12b. These dendrites become unstable and break down to separate hexagonal sheets. These sheets start rolling as shown in Figure 13. After 36 h we observe a mixture of nanorods and nanofibers (Figure 12c). As we provide more time and maintain the

(32) Ribeiro, R. A.; Silva, G. G.; Mohallen, N. D. S. *J. Phys. Chem. Solids* **2001**, *62*, 857.
(33) Lee, J. S.; Volpe, L.; Ribeiro, F. H.; Boudart, M. *J. Catal.* **1988**, *112*, 44.

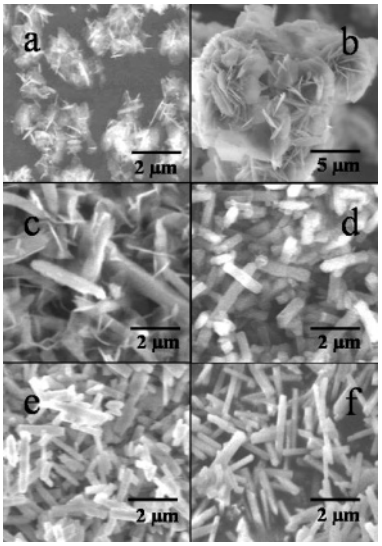

Figure 12. SEM images of the samples taken at regular intervals to find the formation mechanism: (a) 12, (b) 24, (c) 36, (d) 48, (e) 60, and (f) 72 h.

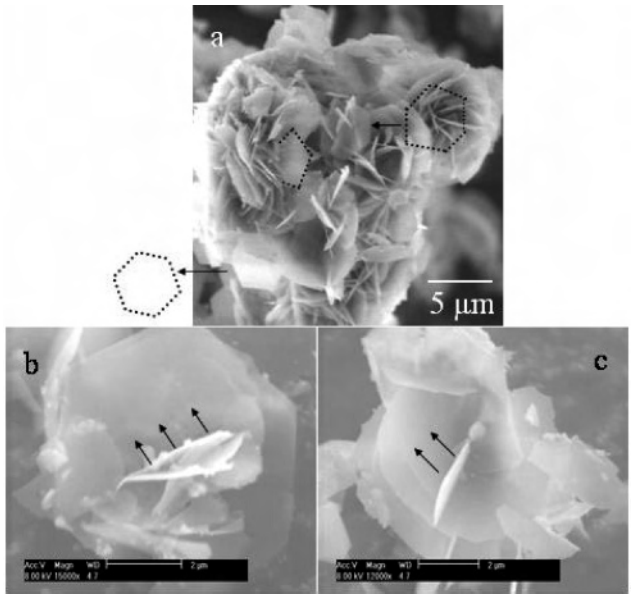

Figure 13. SEM images of a sample treated hydrothermally for 24 h; (a) shows the dendrite-type morphology formed by the hexagonal sheets. Images b and c show the top view of the rolling hexagonal nanosheets; arrows indicate the roll-on direction.

same conditions, these nanofibers disappeared and nanorods grew. After a further increase in time to 48 h the number of nanorods grows significantly as shown in Figure 12d. After 60 h of hydrothermal reaction, the nanorods yield reaches 70−80% as confirmed by SEM in Figure 12e. Finally, after 72 h of reaction, 100% nanorods are obtained as seen in Figure 12f.

We believe that the 1D lithium aluminate nanostructures are formed by a mechanism very much like the rolling up of thin sheets reported by Zhang et al.[34] for lead telluride nanowires. Aluminum oxide nanoparticles would spontaneously dissolve into solution due to a relatively higher free

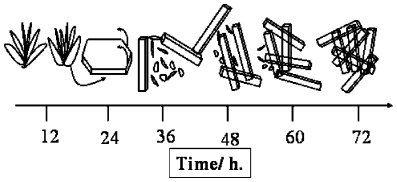

Figure 14. Graphical representation of the events happening during the nanorods formation.

energy compared to that of nanorods under hydrothermal conditions during the first 12 h of reaction. At the same time, the growth units in the solution would diffuse to form the fibrous structures as observed by SEM in Figure 12a. The growth of these structural units leads to lower surface energy forming dendrites having hexagonal sheets as shown in Figure 12b and Figure 13a (indicated by the dotted line). Further hydrothermal treatment under the same conditions makes the dendrites break down, and the formed individual hexagonal sheets start rolling to achieve thermodynamic stability. The nanosheets formed during the early stages of the hydrothermal reaction and the existence of the half-rolled sheet (Figure 13) provides strong evidence for the "rolling-up" mechanism. As we provide more time the sheets rolled-on leading to a small number of nanorods as observed by SEM after 36 h. After 36 h, the reaction seems to be kinetically controlled as nanorods grew at the cost of small fibers and particles. This growth continues until all the fibers or particles vanish, and fully grown nanorods are obtained after 72 h. These entire events of nanorod formation via a roll-on mechanism can be represented schematically on a time scale as shown in Figure 14. The reason to form rectangular nanorods as opposed to the more common cylindrical nanorods is still unclear.[35] We simply assume that as the basic structural unit of our nanorods is orthorhombic β-lithium aluminate, they grow to form an orthorhombic nanostructure.

4. Conclusions

Lithium aluminate nanorods were synthesized by a simple, surfactant-free, hydrothermal method without using any template or catalysts from all-inorganic raw materials. The as-obtained nanorods had orthorhombic β-lithium aluminate structure with rectangular cross section confirmed by XRD, NMR, SEM, and TEM. Various parameters such as lithium precursor, lithium hydroxide to aluminum oxide ratio, hydrothermal temperature, and calcination temperature have crucial effects on the growth of nanorods. The presence of a high concentration of lithium hydroxide (Li/Al = 15), 423 K hydrothermal reaction temperature, and 3 days of reaction time are the prerequisites to obtain fully grown lithium aluminate nanorods with 100% yield. The study on the effect of calcination temperature showed that the morphology of the as-obtained nanorods was fairly well preserved even after calcination at 1273 K for 12 h. Yet, their phase transformed from β-lithium aluminate to γ-lithium aluminate. The nanorods appeared to be formed via a "rolling-up" mechanism.

(34) Zhang, L.; Yu, J. C.; Mo, M.; Wu, L.; Kwong, K. W.; Li, Q. *Small* **2005**, *1*, 349.

(35) Joshi, U. A.; Yoon, S.; Baik, S.; Lee, J. S. *J. Phys. Chem. B* **2006**, *110*, 12249.

Typically 100 g of product was obtained on the lab-scale synthesis. As the method is very simple and we do not use any expensive organic precursor, the scale-up of this process should be very easy for large-scale production.

Acknowledgment. This work has been supported by the Hydrogen R&D center. We appreciate the support of the Korea Ministry of Education and Human Resources Development through the BK 21 program.

Supporting Information Available: SEM images of microbricks and hexagonal sheets. This material is available free of charge via the Internet at http://pubs.acs.org.

IC062227M